*Séminaire Lotharingien de Combinatoire* **85B** (2021)
Article #42, 12 pp.

*Proceedings of the 33rd Conference on Formal Power Series and Algebraic Combinatorics (Ramat Gan)*

# On framed triangulations of flow polytopes, the $\nu$-Tamari lattice and Young's lattice

Matias von Bell[*1], Rafael S. González D'León[†2], Francisco A. Mayorga Cetina[‡2], and Martha Yip[§1]

[1] *Department of Mathematics, University of Kentucky, USA*
[2] *Escuela de Ciencias Exactas e Ingeniería, Universidad Sergio Arboleda, Colombia*

**Abstract.** We study two combinatorially striking triangulations of a family of flow polytopes indexed by lattice paths $\nu$ which we call the $\nu$-caracol flow polytopes. The first triangulation gives a geometric realization of the $\nu$-Tamari complex introduced by Ceballos, Padrol and Sarmiento, whose dual graph is the Hasse diagram of the $\nu$-Tamari lattice introduced by Préville-Ratelle and Viennot. The dual graph of the second triangulation is the Hasse diagram of the principal order ideal determined by $\nu$ in Young's lattice. We use the latter triangulation to show that the $h^*$-vector of the $\nu$-caracol flow polytope is given by the $\nu$-Narayana numbers, extending the result of Mészáros when $\nu$ is a staircase lattice path.

**Keywords:** flow polytope, triangulation, $\nu$-Dyck path, $\nu$-Tamari lattice, Young's lattice

## 1 Introduction

Flow polytopes are a family of beautiful mathematical objects. They appear in optimization theory as the feasible sets in maximum flow problems and they also appear in other areas of mathematics including representation theory and algebraic combinatorics. In this extended abstract, $G = (V, E)$ denotes a *connected directed graph* $G = (V, E)$ with vertex set $V = \{1, 2, \ldots, n+1\}$ and edge multiset $E$ with $m$ edges, with $n, m \in \mathbb{Z}_+$. We assume that any edge $(i, j) \in E$ is directed from $i$ to $j$ whenever $i < j$ and hence $G$ is *acyclic*. At each vertex $i \in V$ we assign a net flow $a_i \in \mathbb{Z}$ satisfying the balance condition $\sum_{i=1}^{n+1} a_i = 0$, and hence $a_{n+1} = -\sum_{i=1}^{n} a_i$. For $\mathbf{a} = (a_1, \ldots, a_n, -\sum_{i=1}^{n} a_i) \in \mathbb{Z}^{n+1}$, an **a**-*flow on* $G$ is a tuple $(x_e)_{e\in E} \in \mathbb{R}^m_{\geq 0}$ such that

$$\sum_{e\in\text{out}(j)} x_e - \sum_{e\in\text{in}(j)} x_e = a_j$$

*matias.vonbell@uky.edu
†rafael.gonzalezl@usa.edu.co
‡f.maycet@gmail.com
§martha.yip@uky.edu. Martha Yip is partially supported by Simons Collaboration Grant 429920.

where $\text{in}(j)$ and $\text{out}(j)$ respectively denote the set of incoming and outgoing edges at $j$, for $j = 1, \ldots, n$. In what follows, by a graph $G$ we mean a connected directed acyclic graph whose sets $\text{out}(1)$, $\text{in}(n+1)$, and $\text{in}(j)$ and $\text{out}(j)$ for $j = 2, \ldots, n$, are not empty. The *flow polytope of $G$ with net flow* $\mathbf{a}$ is the set $\mathcal{F}_G(\mathbf{a})$ of $\mathbf{a}$-flows on $G$. In this article we only consider flow polytopes with unitary flow $\mathbf{a} = \mathbf{e}_1 - \mathbf{e}_{n+1}$, and we will abbreviate the flow polytope of $G$ with unitary flow as $\mathcal{F}_G$. In this case, the only integral points of $\mathcal{F}_G$ are its vertices, which correspond to the unitary flows along maximal directed paths of $G$ from vertex 1 to $n+1$. Such maximal paths are called *routes* (see Figure 4).

A *$d$-simplex* is the convex hull of $d+1$ points in general position in $\mathbb{R}^k$ with $k \geq d$. We say that a $d$-simplex is a *lattice simplex* if all its vertices are in $\mathbb{Z}^k$ and there are no points of $\mathbb{Z}^k$ in its interior. We assume all simplices are lattice simplices. A *(lattice) triangulation* of a $d$-polytope $\mathcal{P}$ is a collection $\mathcal{T}$ of $d$-simplices each of whose vertices are in $\mathcal{P} \cap \mathbb{Z}^d$, such that the union of the simplices in $\mathcal{T}$ is $\mathcal{P}$, and any pair of simplices intersect in a (possibly empty) common face. Since the volume of a $d$-simplex in $\mathbb{R}^d$ is $\frac{1}{d!}$, unimodular triangulations are useful devices to determine the volume of a polytope reducing the calculation to an enumeration problem. The *normalized volume* of a $d$-polytope is defined then as the number of simplices in a unimodular triangulation.

Baldoni and Vergne [2] gave a set of formulas to determine the volume of $\mathcal{F}_G(\mathbf{a})$. These formulas are known as the Lidskii formulas. Mészáros and Morales [10] described a triangulation approach due to Postnikov and Stanley (unpublished), providing an alternative proof of the Lidskii formulas. Together with Striker [11], they combine this strategy with the notion of a *framing* (see Section 3) on a graph introduced by Danilov, Karzanov and Koshevoy in [8]. Different framings of a given graph give different triangulations, giving rise to interesting combinatorial structures on the triangulations. We illustrate this by studying two particular framings on a family of graphs which we call the *$\nu$-caracol graphs* $\text{car}(\nu)$ (see Definition 2.1). These are indexed by lattice paths $\nu$ in $\mathbb{Z}^2$, and generalize work in [5].

The combinatorial structure of a triangulation $\mathcal{T}$ of $\mathcal{F}_G$ associated to a framing of $G$ is encoded in its *dual graph*. This is a graph on the set of simplices in $\mathcal{T}$ with edges between simplices sharing a common facet. In Sections 4 and 5 we discuss two different framings on $\text{car}(\nu)$ which we call the *length* and the *planar* framings. The triangulations arising from these framings have surprising connections to two combinatorial objects that appear in the recent literature:

1. The *$\nu$-Tamari lattice* $\text{Tam}(\nu)$ introduced by Préville-Ratelle and Viennot [12].

2. The principal order ideals $I(\nu)$ in Young's lattice $Y$.

Our main results are the following:

**Theorem 1.1.** *The normalized volume of the flow polytope $\mathcal{F}_{\text{car}(\nu)}$ is given by the number of $\nu$-Dyck paths, that is, the $\nu$-Catalan number* $\text{Cat}(\nu)$.

**Theorem 1.2.** *The length-framed triangulation of $\mathcal{F}_{\mathrm{car}(\nu)}$ is a regular unimodular triangulation whose dual graph is the Hasse diagram of the $\nu$-Tamari lattice* $\mathrm{Tam}(\nu)$*.*

**Theorem 1.3.** *The planar-framed triangulation of $\mathcal{F}_{\mathrm{car}(\nu)}$ is a regular unimodular triangulation whose dual graph is the Hasse diagram of the principal order ideal $I(\nu) \subseteq Y$ in Young's lattice.*

**Theorem 1.4.** *The $h^*$-polynomial of $\mathcal{F}_{\mathrm{car}(\nu)}$ is the $\nu$-Narayana polynomial.*

To describe the combinatorial structure of the triangulations in Theorems 1.2 and 1.3 we use two different $\nu$-Catalan objects. The first is the family of $(I, \overline{J})$-trees introduced by Ceballos, Padrol and Sarmiento in [7] (see Section 4). The second is the family of $\nu$-Dyck paths studied in [12] (see Section 5). We summarize how the combinatorial information in the two triangulations can be read from the corresponding $\nu$-Catalan objects.

| **Triangulation** | **Vertices** | **Simplices** | **Adjacency** | **Dual graph** |
|---|---|---|---|---|
| Length-framed | Arcs of $(I, \overline{J})$-trees | $(I, \overline{J})$-trees | Two $(I, \overline{J})$-trees that differ by one arc | Hasse diag. of $\mathrm{Tam}(\nu)$. |
| Planar-framed | Lattice points above $\nu$ | $\nu$-Dyck paths | Two $\nu$-Dyck paths that differ by a pair EN to NE. | Hasse diag. of $I(\nu)$. |

This extended abstract is organized as follows. In Section 2 we introduce the $\nu$-caracol graph $\mathrm{car}(\nu)$ and its associated flow polytope $\mathcal{F}_{\mathrm{car}(\nu)}$. In Section 3 we describe the context on framed triangulations as presented in [11]. In Section 4 we define the length framing of $\mathrm{car}(\nu)$. We prove Theorem 1.2 and as consequence we conclude that the associated triangulation is a geometric realization of the $\nu$-Tamari complex. In Section 5 we define the planar framing of $\mathrm{car}(\nu)$ and prove Theorem 1.3. As an application, in Section 6 we use the dual graph of the planar-framed triangulation of $\mathcal{F}_{\mathrm{car}(\nu)}$ to obtain the $h^*$-polynomial, which proves Theorem 1.4. This result also gives a new proof that the $h$-vector of the $\nu$-Tamari complex is given by the $\nu$-Narayana numbers.

# 2 The family of $\nu$-caracol flow polytopes

In [5], the second and fourth authors studied the flow polytope of the caracol graph, whose normalized volume is the number of Dyck paths from $(0,0)$ to $(n,n)$, a Catalan number. We now extend this construction.

Let $a, b$ be nonnegative integers, and let $\nu$ be a lattice path from $(0,0)$ to $(b,a)$, consisting of a sequence of $a$ north steps $N = (0,1)$ and $b$ east steps $E = (1,0)$. A *$\nu$-Dyck path* is a lattice path from $(0,0)$ to $(b,a)$ that lies weakly above $\nu$. When $a$ and $b$ are coprime positive integers and $\nu$ is the lattice path that borders the squares which intersect the line $y = \frac{a}{b}x$, this is the special case of the *rational* $(a,b)$*-Dyck path* studied by Armstrong, Loehr and Warrington in [1] who showed that the number of rational $(a,b)$-Dyck paths is the $(a,b)$*-Catalan number* $\mathrm{Cat}(a,b) = \frac{1}{a+b}\binom{a+b}{a}$. When $(a,b) = (n,n+1)$, this is the case of the classical Catalan number $\mathrm{Cat}(n) = \frac{1}{2n+1}\binom{2n+1}{n} = \frac{1}{n+1}\binom{2n}{n}$. For general $\nu$, the number $\mathrm{Cat}(\nu)$ of $\nu$-Dyck paths can be calculated by a determinantal formula, but no closed-form positive formula is known. For more on $\nu$-Dyck paths, see for example Ceballos and González D'León [6], or Préville-Ratelle and Viennot [12].

**Definition 2.1.** Let $a, b$ be nonnegative integers, and let $\nu$ be a lattice path from $(0,0)$ to $(b,a)$ where $\nu = NE^{\nu_1}NE^{\nu_2}\cdots NE^{\nu_a}$. The *$\nu$-caracol graph* $\mathrm{car}(\nu)$ is the graph on the vertex set $[a+3]$, together with $\nu_i$ copies of the edge $(1, i+2)$ for $i = 1,\ldots,a$, the edges $(i, a+3)$ for $i = 2,\ldots,a+1$, and the edges $(i,i+1)$ for $i = 1,\ldots,a+2$.

Note that in this construction, the graph $\mathrm{car}(\nu)$ has $n+1 := a+3$ vertices, and the in-degree $\mathrm{in}_i$ of the vertex $i$ in $\mathrm{car}(\nu)$ is $\mathrm{in}_2 = 1$, $\mathrm{in}_i = \nu_{i-2}+1$ for $i = 3,\ldots,n$ and $\mathrm{in}_{n+1} = n-1$. The number of edges $m$ of $\mathrm{car}(\nu)$ is computed by summing the in-degrees of its vertices, so that $m = \sum_{i=2}^{n+1} \mathrm{in}_i = 1 + \sum_{i=1}^{a}(\nu_i+1) + (a+1) = 2a+b+2$. We can conclude from this that $\dim \mathcal{F}_{\mathrm{car}(\nu)} = m - n = a+b$.

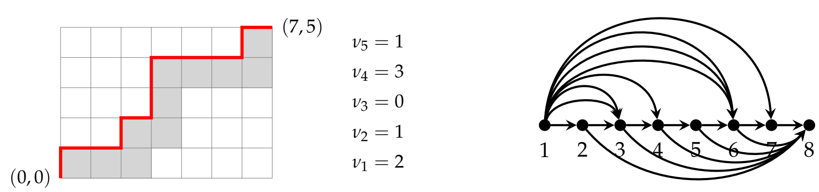


**Figure 1:** A lattice path $\nu = NE^2NE^1NE^0NE^3NE^1$ and its $\nu$-caracol graph $\mathrm{car}(\nu)$.

Mészáros and Morales [10, Corollary 6.17] have previously considered the flow polytope $\mathcal{F}_{\mathrm{car}(\nu)}$ (denoted $\Pi_a^*(\nu)$ in their work), where they observed that its normalized volume is the number of lattice points in the Pitman–Stanley polytope $\Pi_a(\nu) = \{\mathbf{y} \in \mathbb{R}^a \mid \sum_{i=1}^{k} y_i \leq \sum_{i=1}^{k} \nu_i\}$, which is equal to the number of $\nu$-Dyck paths. We obtain a proof of this result by giving a combinatorial interpretation to the vector partitions enumerated by the Kostant partition function in the Lidskii volume formula. This method was first considered in [5]. We refer the reader to the full article [3] for the details of the proof.

**Theorem 1.1.** *The normalized volume of the flow polytope* $\mathcal{F}_{\mathrm{car}(\nu)}$ *is given by the number of $\nu$-Dyck paths, that is, the $\nu$-Catalan number* $\mathrm{Cat}(\nu)$.

See Sections 4 and 5 for two geometric proofs of this result.

# 3 Framed triangulations of a flow polytope

We now describe the family of triangulations defined by Danilov, Karzanov, and Koshevoy [8], interpreted as special cases of the Postnikov–Stanley triangulations described by Mészáros, Morales and Striker in [11].

We call *inner vertices* the vertices $\{2, \ldots, n\}$ of a graph $G$ on $n+1$ vertices. A *framing* at the inner vertex $i$ is a pair of linear orders $(\prec_{\text{in}(i)}, \prec_{\text{out}(i)})$ on the incoming and outgoing edges at $i$. A *framed graph*, denoted $(G, \prec)$, is a graph with a framing at every inner vertex. In Sections 4 and 5, we will consider two specific framings of the caracol graphs $\text{car}(\nu)$, which lead to combinatorially interesting triangulations of $\mathcal{F}_{\text{car}(\nu)}$. An example of these two framings at a vertex is given in Figure 2.

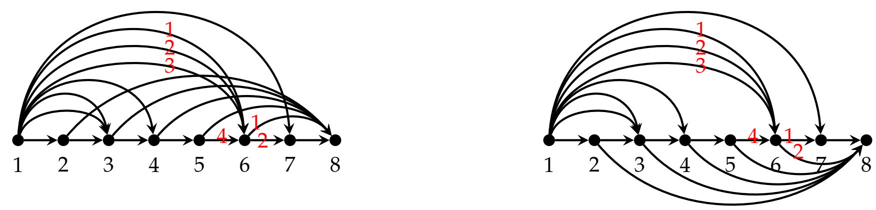


**Figure 2:** Length (left) and planar (right) framings at the vertex 6 of $G = \text{car}(\nu)$. The embedding of the graph on the right highlights the planarity of $G$.

For an inner vertex $i$ of a graph $G$, let $\text{In}(i)$ and $\text{Out}(i)$ respectively denote the set of maximal paths ending at $i$ and the set of maximal paths beginning at $i$. For a route $R$ containing an inner vertex $i$, let $Ri$ (respectively $iR$) denote the maximal subpath of $R$ ending (respectively beginning) at $i$. Define linear orders $\prec_{\text{In}(i)}$ and $\prec_{\text{Out}(i)}$ on $\text{In}(i)$ and $\text{Out}(i)$ as follows. Given paths $R, Q \in \text{In}(i)$, let $j \leq i$ be the smallest vertex after which $Ri$ and $Qi$ coincide. Let $e_R$ be the edge of $R$ entering $j$ and let $e_Q$ be the edge of $Q$ entering $j$. Then $R \prec_{\text{In}(i)} Q$ if and only if $e_R \prec_{\text{in}(j)} e_Q$. Similarly for $R, Q \in \text{Out}(i)$, let $j \geq i$ be the largest vertex before which $iR$ and $iQ$ coincide. Then $R \prec_{\text{Out}(i)} Q$ if and only if $e_R \prec_{\text{out}(j)} e_Q$.

Two routes $R$ and $Q$ containing an inner vertex $i$ are *coherent at* $i$ if $Ri$ and $Qi$ are ordered the same as $iR$ and $iQ$. Routes $R$ and $Q$ are *coherent* if they are coherent at each common inner vertex. A set of mutually coherent routes is a *clique*. For a maximal clique $C$, let $\Delta_C$ denote the convex hull of the vertices of $\mathcal{F}_G$ corresponding to the unitary flows along the routes in $C$.

**Proposition 3.1** (Danilov et al. [8]). *Let $(G, \prec)$ be a framed graph. Then*

$$\{\Delta_C \mid C \text{ is a maximal clique of } (G, \prec)\}$$

*is the set of the top dimensional simplices in a regular unimodular triangulation of $\mathcal{F}_G$.*

# 4 The length-framed triangulation and the $\nu$-Tamari lattice

We show that the flow polytope $\mathcal{F}_{\mathrm{car}(\nu)}$ has a regular unimodular triangulation whose dual graph structure is given by the Hasse diagram of the $\nu$-Tamari lattice.

## 4.1 The $\nu$-Tamari lattice

The $\nu$-Tamari lattice was introduced by Préville-Ratelle and Viennot [12, Theorem 1] as a partial order on the set of $\nu$-Dyck paths. Ceballos, Padrol and Sarmiento [7] showed that the $\nu$-Tamari lattice $\mathrm{Tam}(\nu)$ is the one-skeleton of a polyhedral complex known as the $\nu$-associahedron $K_\nu$, which generalizes the classical associahedron. In their article, they gave a description of the faces of $K_\nu$ in terms of covering $(I,\overline{J})$-forests. In [4], the first and fourth authors gave additional combinatorial interpretations of the face poset of $K_\nu$ in terms of $\nu$-Schröder paths and $\nu$-Schröder trees.

Let $I \sqcup \overline{J}$ be a partition of $[N]$ such that $1 \in I$ and $N \in \overline{J}$. An $(I,\overline{J})$-*forest* is a subgraph of the complete bipartite graph $K_{|I|,|\overline{J}|}$ that is *increasing*, that is, each arc $(i,\overline{j})$ satisfies $i < \overline{j}$, and *non-crossing*, so that the graph does not contain arcs $(i,\overline{j})$ and $(i',\overline{j}')$ with $i < i' < j < \overline{j}'$. An $(I,\overline{J})$-*tree* is a maximal $(I,\overline{J})$-forest. To a pair $(I,\overline{J})$ we can associate a unique lattice path $\nu$ as follows. Assign to the elements in $I$ and $\overline{J}$ the labels $E$ and $N$ respectively. Reading the labels of the nodes $k = 2,\ldots,N-1$ in increasing order yields a lattice path $\nu$ from $(0,0)$ to $(|I|-1,|\overline{J}|-1)$. See Figure 3 for an example. Conversely, a lattice path $\nu$ determines a unique pair $(I,\overline{J})$, and hence a unique set of $(I,\overline{J})$-trees. Let $\mathcal{T}_\nu$ denote the set of $(I,\overline{J})$-trees determined by $\nu$.

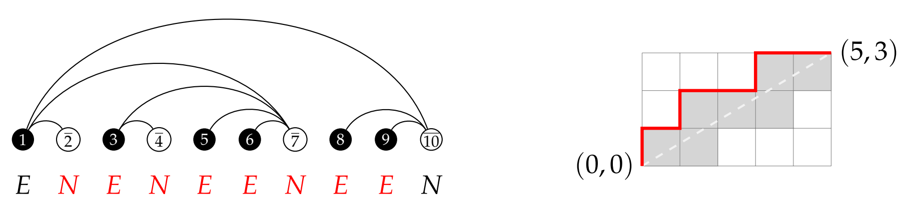


**Figure 3:** An $(I,\overline{J})$-tree with $I = \{1,3,5,6,8,9\}$ and $\overline{J} = \{2,4,7,10\}$ (left), and the corresponding lattice path $\nu = NENE^2NE^2$ (right).

**Proposition 4.1** (Ceballos et al. [7])**.** *The Hasse diagram of the $\nu$-Tamari lattice is the graph whose vertices are the $(I,\overline{J})$-trees determined by $\nu$, with edges between $(I,\overline{J})$-trees that differ by exactly one arc.*

See Figure 6 for an illustration of the $\nu$-Tamari lattice for $\nu = NENE^2NE^2$ with vertices indexed by $(I,\overline{J})$-trees.

## 4.2 The length-framed triangulation

In this section we study the length-framed triangulation of $\mathcal{F}_{\mathrm{car}(\nu)}$. To define the framing we need to be able to distinguish between the multiedges. To that end, we label multiedges between two vertices from top to bottom in the embedding with increasing natural numbers.

**Definition 4.2.** Let $G$ be a graph on the vertex set $\{1,\dots,n+1\}$. Define the *length* of a directed edge $(i,j)$ to be $j-i$. Given an inner vertex $i \in [2,n]$ of $G$, the *length framing* for $G$ at $i$ is the pair of linear orders $(\prec_{\mathrm{in}(i)}, \prec_{\mathrm{out}(i)})$ where longer edges precede shorter edges and multiedges with smaller labels precede ones with larger labels. Figure 2 gives an example of the length framing of $\mathrm{car}(\nu)$ with $\nu = NE^2NENNE^3NE$.

Recall that the vertices (unitary flows) of $\mathcal{F}_{\mathrm{car}(\nu)}$ are determined by routes in $\mathrm{car}(\nu)$. These are completely characterized by two edges: the initial edge that is of the form $(1, j+1)$ with label $i$, and the terminal edge that is of the form $(\ell+1, n+1)$ (which always has label $i = 1$) with $1 \le j \le \ell < n$. We denote such a route by $R_{j,i,\ell}$.

**Lemma 4.3.** *The set of routes $\mathcal{R}_\nu$ in the $\nu$-caracol graph* $\mathrm{car}(\nu)$ *is in bijection with the set $\mathcal{A}_\nu$ of possible arcs in the $(I,\overline{J})$-trees in $\mathcal{T}_\nu$.*

*Outline of proof.* We define a map $\varphi : \mathcal{R}_\nu \to \mathcal{A}_\nu$. The elements in the sets $I$ and $\overline{J}$ respectively correspond to the $N$ and $E$ steps in the path $\overline{\nu} = E\nu N$, as in Figure 3. Describing the bijection in terms of the $N$ and $E$ steps is easier than using the elements of $I$ and $\overline{J}$, so we add indices to the $N$ and $E$ steps in order to distinguish between them. First index the $j$-th $N$ step in $\overline{\nu}$ by $j$, then index each $E$ with a pair $(j,i)$ where $j$ is index of the next $N_j$ in $\overline{\nu}$, and $i$ is the number of steps taken to reach $N_j$. Now, arcs in the $(I,\overline{J})$-trees in $\mathcal{T}_\nu$ can be expressed as pairs of the form $(E_{j,i}, N_\ell)$. Recall that the routes in $\mathrm{car}(\nu)$ are of the form $R_{j,i,\ell}$. We define the map by $\varphi(R_{j,i,\ell}) = (E_{j,i}, N_\ell)$. Figure 4 shows an example of this correspondence between routes and arcs. We refer the reader to the full article [3] for the proof that $\varphi$ is a bijection. □

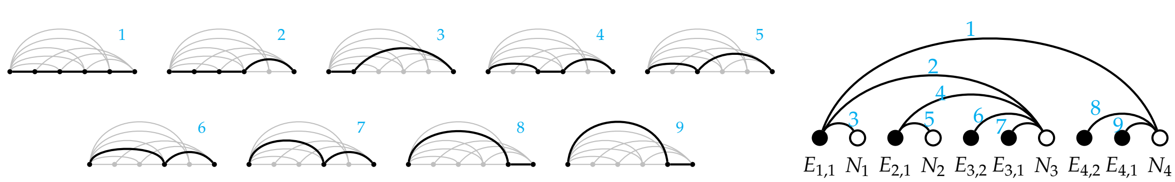


**Figure 4:** A maximal clique of routes (left) representing a simplex in the length-framed triangulation of $\mathcal{F}_{\mathrm{car}(\nu)}$ for $\nu = NENE^2NE^2$. The bijection $\varphi$ of Lemma 4.3 sends this clique to the $(I,\overline{J})$-tree on the right.

**Lemma 4.4.** *Let $\prec$ denote the length framing, and let $\varphi$ be the bijection in Lemma 4.3. Two routes $R_{j,i,\ell}$ and $R_{j',i',\ell'}$ in the framed graph $(\mathrm{car}(\nu), \prec)$ are coherent if and only if $\varphi(R_{j,i,\ell}) = (E_{j,i}, N_\ell)$ and $\varphi(R_{j',i',\ell'}) = (E_{j',i'}, N_{\ell'})$ are non-crossing arcs in $\mathcal{A}_\nu$.*

*Outline of proof.* We can assume without loss of generality that $\ell < \ell'$ (if $\ell = \ell'$, the arcs are non-crossing and the routes are coherent). There are two ways in which the arcs $\varphi(R_{j,i,\ell})$ and $\varphi(R_{j',i',\ell'})$ can cross: (1) when $j < j'$, or (2) when $j = j'$ with $i' < i$. In both cases $R_{j,i,\ell}$ and $R_{j',i',\ell'}$ are incoherent at the vertex $j'$. Conversely, if $R_{j,i,\ell}$ and $R_{j',i',\ell'}$ are incoherent, they must be incoherent at a minimal vertex $j'$. Thus either $j < j'$ or $j = j'$ with $i' < i$, which are precisely the ways in which $\varphi(R_{j,i,\ell})$ and $\varphi(R_{j',i',\ell'})$ can cross. □

**Theorem 1.2.** *The length-framed triangulation of $\mathcal{F}_{\mathrm{car}(\nu)}$ is a regular unimodular triangulation whose dual graph is the Hasse diagram of the $\nu$-Tamari lattice* $\mathrm{Tam}(\nu)$*.*

*Proof.* By Lemma 4.4, the bijection $\varphi$ in Lemma 4.3 extends to a bijection $\Phi$ from the set of maximal cliques of routes in the length-framed $\mathrm{car}(\nu)$ to the set $\mathcal{T}_\nu$ of $(I, \overline{J})$-trees determined by $\nu$. Two simplices in a DKK triangulation of a flow polytope are adjacent if and only if they differ by a single vertex, that is, if the corresponding maximal cliques differ by a single route. Under the bijection $\Phi$, two simplices are adjacent if and only if their corresponding $(I, \overline{J})$-trees differ by a single arc, which is precisely the description of the cover relations in the $\nu$-Tamari lattice. □

**Example 4.5.** Let $\nu = NENE^2NE^2$. The bijection $\Phi$ between cliques of routes of $\mathrm{car}(\nu)$ and $(I, \overline{J})$-trees is shown in Figure 4. The dual graph of the length-framed triangulation of $\mathcal{F}_{\mathrm{car}(\nu)}$ is shown in Figure 6 (left).

In [7] Ceballos, Padrol and Sarmiento introduced the $(I, \overline{J})$-*Tamari complex* $\mathcal{A}_{I,\overline{J}}$ as the flag simplicial complex on $\{(i, \bar{j}) \in I \times \overline{J} \mid i < \bar{j}\}$ whose minimal non-faces are the pairs $\{(i, \bar{j}), (i', \bar{j}')\}$ with $i < i' < j < j'$, that is, the complex on collections of non-crossing arcs of $(I, \overline{J})$-trees. The following is then a corollary of Theorem 1.2.

**Corollary 4.6.** *Let $\nu$ be the lattice path in the grid $(0, 0)$ to $(b, a)$ associated to the pair $(I, \overline{J})$. The length-framed triangulation of $\mathcal{F}_{\mathrm{car}(\nu)}$ is a geometric realization of the $(I, \overline{J})$-Tamari complex of dimension $a + b$ in $\mathbb{R}^{2a+b+2}$.*

**Remark 4.7.** A simple projection of the coordinates along the edges of the form $(i, i + 1)$ produces a lower dimensional geometric realization of the $(I, \overline{J})$-Tamari complex in $\mathbb{R}^{a+b}$. This geometric realization is integrally equivalent to the first of three realizations given in [7, Theorem 1.1].

# 5 The planar-framed triangulation and Young's lattice

We show that the flow polytope $\mathcal{F}_{\mathrm{car}(\nu)}$ has a regular unimodular triangulation whose dual graph structure is given by the Hasse diagram of the principal order ideal $I(\nu)$ in Young's lattice.

## 5.1 Principal order ideals in Young's lattice

Recall that *Young's lattice* $Y$ is the poset on integer partitions $\lambda$ with cover relations $\lambda \succ \lambda'$ if $\lambda$ is obtained from $\lambda'$ by removing one corner box of $\lambda'$. Note that a lattice path $\nu$ in the rectangular grid defined by $(0,0)$ to $(b,a)$ defines a partition $\lambda(\nu) = (\lambda_1, \dots, \lambda_a)$ by letting $\lambda_k = b - \sum_{i=a-k+1}^{a} \nu_i$ for $k = 1, \dots, a$. The Young diagram for $\lambda(\nu)$ may be visualized as the region within the rectangle from $(0,0)$ to $(b,a)$ which lies NW of $\nu$, see Figure 6 for an example. An *order ideal* of a poset $P$ is a subset $I \subseteq P$ with the property that if $x \in I$ and $y \leq x$, then $y \in I$. An ideal is said to be *principal* if it has a single maximal element $x \in P$, and such an ideal will be denoted by $I(x)$.

If $\mu$ is a $\nu$-Dyck path, then it lies weakly above the path $\nu$ and so $\mu$ can be identified with a partition $\lambda(\mu)$ that is contained in $\lambda(\nu)$. Thus there is a one-to-one correspondence between the set of $\nu$-Dyck paths with the set of elements in the order ideal $I(\nu) := I(\lambda(\mu))$ in $Y$. Under this correspondence, in terms of $\nu$-Dyck paths, a path $\pi$ covers a path $\mu$ if and only if $\pi$ can be obtained from $\mu$ by replacing a consecutive $NE$ pair by a $EN$ pair. See Figure 6 for an example of $I(\nu)$ with $\nu = NENE^2NE^2$.

## 5.2 The planar-framed triangulation

**Definition 5.1.** Let $G$ be a planar graph that affords a planar embedding in the plane such that if vertex $i$ is at the coordinates $(x_i, y_i)$, then $x_i < x_j$ for all $i < j$. This leads to natural orderings $(\prec_{\mathrm{in}(i)}, \prec_{\mathrm{out}(i)})$ at every inner vertex $i$ of $G$ as follows: with respect to the planar embedding of $G$, the incoming edges at the vertex $i$ are ordered in increasing order from the top to the bottom, and the same for the outgoing edges from the vertex $i$. This is the *planar framing* for $G$. Figure 2 gives an example of the planar framing of $\mathrm{car}(\nu)$ with $\nu = NE^2NENNE^3NE$.

**Lemma 5.2.** *Let $\nu$ be a lattice path from $(0,0)$ to $(b,a)$. The set of routes $\mathcal{R}_\nu$ in the $\nu$-caracol graph* $\mathrm{car}(\nu)$ *is in bijection with the set of lattice points $\mathcal{L}_\nu$ in the rectangle defined by $(0,0)$ and $(b,a)$ that lie weakly above the lattice path $\nu$.*

*Outline of proof.* We fix an embedding of $\mathrm{car}(\nu)$ in the plane so that the path $(1, \dots, n+1)$ lies on the $x$-axis. Define a map $\psi : \mathcal{R}_\nu \to \mathcal{L}_\nu$ by $\psi(R) = (j, \ell)$ where $j$ is the number of bounded faces of $\mathrm{car}(\nu)$ that lie below $R$ and above the $x$-axis, and $\ell$ is the number of bounded faces that lie below $R$ and the $x$-axis. See Figure 5 for an example. We refer the reader to the full article [3] for the proof that $\psi$ is a bijection. □

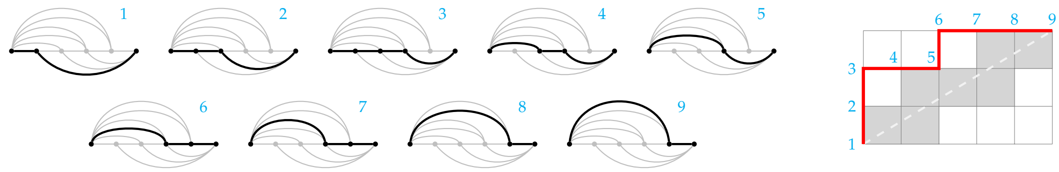

**Figure 5:** A maximal clique of routes (left) representing a simplex in the planar-framed triangulation of $\mathcal{F}_{\text{car}(\nu)}$ for $\nu = NENE^2NE^2$. The bijection $\psi$ of Lemma 5.2 sends this clique to the $\nu$-Dyck path on the right.

Given two lattice points $(x_1, y_1)$ and $(x_2, y_2)$, we say that they are *incompatible* if $y_1 < y_2$ and $x_1 > x_2$. They are *compatible* otherwise. Maximal sets of compatible lattice points lying above $\nu$ determine a $\nu$-Dyck path.

**Lemma 5.3.** *Let $\prec$ denote the planar framing, and let $\psi$ be the bijection in Lemma 5.2. Two routes $R_1$ and $R_2$ in the framed graph $(\text{car}(\nu), \prec)$ are coherent if and only if $\psi(R_1)$ and $\psi(R_2)$ are compatible.*

*Proof.* A result of Mészáros, Morales and Striker [11, Lemma 6.5] states that two routes in a planar framing of a graph $G$ are coherent if and only if they are non-crossing in $G$. If $R_1$ and $R_2$ are two coherent routes in $\text{car}(\nu)$ such that $\ell_1 < \ell_2$, then the fact that $R_1$ and $R_2$ are non-crossing implies that $j_1 \leq j_2$. □

**Theorem 1.3.** *The planar-framed triangulation of $\mathcal{F}_{\text{car}(\nu)}$ is a regular unimodular triangulation whose dual graph is the Hasse diagram of the principal order ideal $I(\nu) \subseteq Y$ in Young's lattice.*

*Outline of proof.* By Lemma 5.3, the bijection $\psi$ in Lemma 5.2 extends to a bijection $\Psi$ from maximal cliques of routes in the planar-framed $\text{car}(\nu)$ to maximal set of compatible lattice points lying above $\nu$, which are $\nu$-Dyck paths. Two simplices in a DKK triangulation of a flow polytope are adjacent if and only if they differ by a single vertex. Under the bijection $\Psi$, two simplices are adjacent if and only if their corresponding $\nu$-Dyck paths differ by the transposition of a consecutive $NE$ pair, which is precisely the description of the cover relation in $I(\nu)$. □

**Example 5.4.** Let $\nu = NENE^2NE^2$. The bijection $\Psi$ between cliques of routes of $\text{car}(\nu)$ and $\nu$-Dyck paths is shown in Figure 5. The dual graph of the planar-framed triangulation of $\mathcal{F}_{\text{car}(\nu)}$ is shown in Figure 6 (right).

A special case when the dual graphs of the length-framed and planar-framed triangulations of $\mathcal{F}_{\text{car}(\nu)}$ are the same is given by the following proposition.

**Proposition 5.5.** *When $\nu = E^aN^b$, so that the set of $\nu$-Dyck paths is the set of all lattice paths from $(0,0)$ to $(b, a)$, the length-framed triangulation and the planar-framed triangulation of $\mathcal{F}_{\text{car}(\nu)}$ have the same dual structure.*

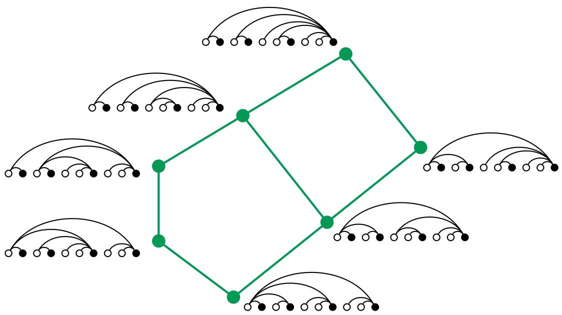

**Figure 6:** The $\nu$-Tamari lattice indexed by $(I, \overline{J})$-trees (left) and the order ideal $I(\nu) \subseteq Y$ indexed by $\nu$-Dyck paths (right) for $\nu = NENE^2NE^2$. These are the dual graphs of the length-framed and planar-framed triangulations of $\mathcal{F}_{\mathrm{car}(\nu)}$.

# 6 The $h^*$-vector of the $\nu$-caracol flow polytope

It is well-known that the $h^*$-vector of an integral polytope equals the $h$-vector of any of its shellable regular unimodular triangulations (see [3] for these definitions), so we compute the $h$-vector of the planar-framed triangulation of $\mathcal{F}_{\mathrm{car}(\nu)}$, extending a result of Mészáros [9, Theorem 4.4] in the classical case.

Let $\nu$ be a lattice path from $(0,0)$ to $(b,a)$. For $i = 0,\dots,a$, the *$\nu$-Narayana number* $\mathrm{Nar}_\nu(i)$ is the number of $\nu$-Dyck paths with $i$ valleys, where a *valley* is a consecutive $EN$ pair. The *$\nu$-Narayana polynomial* is $N_\nu(x) = \sum_{i \geq 0} \mathrm{Nar}_\nu(i) x^i$.

**Theorem 1.4.** *The $h^*$-polynomial of $\mathcal{F}_{\mathrm{car}(\nu)}$ is the $\nu$-Narayana polynomial.*

*Outline of proof.* Any linear extension of the order ideal $I(\nu)$ gives a shelling order of the planar-framed triangulation of $\mathcal{F}_{\mathrm{car}(\nu)}$. The $h$-vectors of shellable simplicial complexes have non-negative entries which can be computed from the shelling order on its facets as follows. For a fixed shelling order $F_1, \dots, F_s$, the restriction of the facet $F_j$ is defined as $R_j := \{v \text{ a vertex in } F_j : F_j \backslash v \subseteq F_i \text{ for some } i < j\}$. Then the $i$-th entry of the $h$-vector is

$$\begin{aligned} h_i &= |\{j : |R_j| = i, 1 \leq j \leq s\}| = |\{\text{paths in } I(\nu) \text{ that cover exactly } i \text{ paths}\}| \\ &= |\{\nu\text{-Dyck paths with exactly } i \text{ valleys}\}| = \mathrm{Nar}_\nu(i). \end{aligned}$$ □

A different proof of Theorem 1.4 can be obtained by computing the $h$-vector of the length-framed triangulation of $\mathcal{F}_{\mathrm{car}(\nu)}$, which by Corollary 4.6 is combinatorially equivalent to the $(I, \overline{J})$-Tamari complex with the pair $(I, \overline{J})$ associated to $\nu$, which we also call the *$(I, \overline{J})$-Tamari complex*. In [7, Lemma 4.5] a shelling order on facets of this complex was used to show that the $h$-vector of the $(I, \overline{J})$-Tamari complex is given by the $\nu$-Narayana numbers. Since any shellable regular unimodular triangulation can be used to calculate the $h^*$-vector of $\mathcal{F}_{\mathrm{car}(\nu)}$, Theorem 1.4 provides a new proof that the $h$-vector of the $(I, \overline{J})$-Tamari complex is given by the $\nu$-Narayana numbers.

## Acknowledgements

We are extremely grateful to AIM and the SQuaRE group "Computing volumes and lattice points of flow polytopes" as some of the ideas of this work came from discussions within the group. In particular, we want to thank Alejandro Morales for the many enlightening discussions and explanations on triangulations of flow polytopes.

## References

[1] D. Armstrong, N. A. Loehr, and G. S. Warrington. "Rational parking functions and Catalan numbers". *Ann. Comb.* **20**.1 (2016), pp. 21–58.

[2] W. Baldoni and M. Vergne. "Kostant partitions functions and flow polytopes". *Transform. Groups* **13**.3-4 (2008), pp. 447–469.

[3] M. von Bell, R. S. González D'León, F. A. Mayorga Centina, and M. Yip. "A unifying framework for the $\nu$-Tamari lattice and principal order ideals in Young's lattice". 2021. arXiv:2101.10425.

[4] M. von Bell and M. Yip. "Schröder combinatorics and $\nu$-associahedra". 2020. arXiv: 2006.09804.

[5] C. Benedetti, R. S. González D'León, C. R. H. Hanusa, P. E. Harris, A. Khare, A. H. Morales, and M. Yip. "A combinatorial model for computing volumes of flow polytopes". *Trans. Amer. Math. Soc.* **372**.5 (2019), pp. 3369–3404.

[6] C. Ceballos and R. S. González D'León. "Signature Catalan combinatorics". *J. Comb.* **10**.4 (2019), pp. 725–773.

[7] C. Ceballos, A. Padrol, and C. Sarmiento. "Geometry of $\nu$-Tamari lattices in types $A$ and $B$". *Trans. Amer. Math. Soc.* **371**.4 (2019), pp. 2575–2622.

[8] V. I. Danilov, A. V. Karzanov, and K. G. A. "Coherent fans in the space of flows in framed graphs". Discrete Math. Theor. Comput. Sci. Proc., AR. 2012, pp. 481–490.

[9] K. Mészáros. "Pipe dream complexes and triangulations of root polytopes belong together". *SIAM J. Discrete Math.* **30**.1 (2016), pp. 100–111.

[10] K. Mészáros and A. H. Morales. "Volumes and Ehrhart polynomials of flow polytopes". *Math. Z.* **293**.3-4 (2019), pp. 1369–1401.

[11] K. Mészáros, A. H. Morales, and J. Striker. "On flow polytopes, order polytopes, and certain faces of the alternating sign matrix polytope". *Discrete Comput. Geom.* **62**.1 (2019), pp. 128–163.

[12] L.-F. Préville-Ratelle and X. Viennot. "The enumeration of generalized Tamari intervals". *Trans. Amer. Math. Soc.* **369**.7 (2017), pp. 5219–5239.